Thermal Science and Engineering 2024, 7(1), 6036.
https://doi.org/10.24294/tse.v7i1.6036

Article

Thermal radiation and MHD effect on the double-diffusive convective flow of second-grade fluid over a stretching sheet

K. G. Chandan, B. Patil Mallikarjun*

Department of Studies and Research in Mathematics, Tumkur University, Tumakuru 572103, India
*** Corresponding author:** B. Patil Mallikarjun, mbp1007@yahoo.com

CITATION

Chandan KG, Mallikarjun BP. Thermal radiation and MHD effect on the double-diffusive convective flow of second-grade fluid over a stretching sheet. Thermal Science and Engineering. 2024; 7(1): 6036. https://doi.org/10.24294/tse.v7i1.6036

ARTICLE INFO

Received: 17 December 2023
Accepted: 9 January 2024
Available online: 18 January 2024

Abstract: An investigation is conducted into how radiation affects the non-Newtonian second-grade fluid in double-diffusive convection over a stretching sheet. When fluid is flowing through a porous material, the Lorentz force and viscous dissipation are also taken into account. The flow equations are coupled partial differential equations that can be solved by MATLAB's built-in bvp4c algorithm after being transformed into ODEs using appropriate similarity transformations. Utilizing graphs and tables, the impact of a flow parameter on a fluid is displayed. On velocity, temperature, and concentration profiles, the effects of the magnetic field, Eckert number, and Schmidt number have been visually represented. Calculate their inaccuracy by comparing the Nusselt number and Sherwood number values to those from earlier investigations.

Keywords: magnetic field; double diffusion; porous medium; second-grade fluid; stretching sheet

1. Introduction

The models of Misra et al. [1] and Jacobson and Hamrock [2] are among those that have been developed to examine the behavior of non-Newtonian fluids. Due to its use in engineering and industrial purposes, fluid flow problems over a stretching/shrinking surface are attracting the interest of many researchers. Crane [3] later developed this work for flow past a stretching sheet after Sakiadis [4,5] had first studied the problem of a stretching sheet. Many famous scholars have been solving the majority of stretching sheet problems analytically for decades. In the papers of Hamad [6], Wang [7], Khan et al. [8], Hayat et al. [9], flow problems are solved analytically by taking into account the magnetic field in natural convection of nanofluid, surface slip and suction due to stretching sheet, three-dimensional flow over a non-linearly stretching sheet, and magnetohydrodynamics (MHD) in Oldroyd-B nanofluid, respectively. Stretching sheet problems can also be solved numerically using a variety of methods; current research has compared these numerical approaches to their analytical counterparts. When comparing the prominent Chebyshev pseudospectral and finite difference methods, Tzirtzilakis and Tanoudis [10] take into account the movement of biomagnetic fluid flow over a stretching sheet. In their contribution, Datti et al. [11] compare the analytical solution with the fourth-order Runge-Kutta method while accounting for MHD and heat radiation across a non-isothermal stretched sheet.

In recognition of its applications in oceanography [12], geology, and astrophysics, double-diffusive convection has recently attracted the attention of many academics. Turner [13,14] first used the term "double diffusion" to describe

the phenomenon of diffusion caused by two distinct density gradients in a fluid. Many non-Newtonian fluids, including Williamson and Casson fluids, are subject to double-diffusive convection; in this case, we are applying this convection phenomenon to a non-Newtonian second-grade fluid that has nonlinear properties. Second-grade fluid flowing through a porous channel in the presence of a uniform magnetic field that is applied in the transverse direction of flow is solved using the homotopy analysis method by Hayat et al. [15]. Vajravelu and Rollins [16] utilized a uniform magnetic field over a stretching sheet to solve the momentum problem analytically and quantitatively. Bafakeeh et al. [17] explored the unsteady condition of second-grade fluid by taking into account thermal radiation and chemical reactions along with analyzing the physical quantities. The papers of Massoudi and Vaidya [18], Gowda et al. [19], Awan et al. [20], and Khan et al. [21] list several works on second-grade fluid.

One of the three main mechanisms of heat transfer is thermal radiation; the other two mechanisms are convection and radiation. Due to the thermal motion of particles in fluid, electromagnetic radiation is generated, which is recurrently known as thermal radiation. The essence of different Newtonian/non-Newtonian fluids can be studied by applying the effect of thermal radiation. The effect of thermal radiation along with a magnetic field due to the double-diffusive peristaltic flow of a nanofluid in a porous medium was extensively studied by Kotnurkar and Giddaiah [22], Asha and Sunitha [23], and Asha and Sunitha [24]. In the study of Akbar et al. [25], entropy is taken into account by considering radiation and inclined MHD effects for two different fluids, such as Newtonian and Williamson fluids, as interpreted by Dadheech et al.

The primary development of our study is to apply thermal radiation to the double-diffusive convection of second-grade fluid flowing through a porous medium. The study of second-grade fluid flowing over a stretching sheet was recently published in papers by Dey and Borah [26], Ghadikolaei et al. [27], and Endalew and Sarkar [28]. The governing equations of flow are partial differential equations that can be transformed into ordinary differential equations using suitable similarity transformations and solved numerically using the MATLAB bvp4c technique. Results have been shown through graphs and compared with the values in tables with previous studies of second-grade fluid, and error will be calculated for the Nusselt number.

2. Formulation of the problem

The laminar flow of fluid is imprisoned in the region $x > 0$ and $y > 0$ when the incompressible flow of a nonlinear second-grade fluid via a stretched surface is taken into account. Because of the double-diffusion, the lower end is either heated or cooled, and two separate density gradients result from the additional substance. Temperature and concentration are symbolized by T and C, respectively, while wall temperature and concentration are represented by T_w and C_w. When heated, the fluid has a temperature of $T_w > T_\infty$ (ambient state), and when cooled, it has a temperature of $T_w < T_\infty$. The sheet behaves as an elastic surface with a velocity of $u_w(x) = cx$, and a uniform magnetic field B_0 applied perpendicular to the direction of fluid flow.

Constant $c > 0$ signifies surface stretch.

If T is the Cauchy stress tensor, then the equations constituting for non-Newtonian second-grade fluid model is given by [28]:

$$T = -pI + \sum_{j=1}^{2} S_j \tag{1}$$

where I is the identity tensor, p is the pressure and S_j is the extra stress tensor, such that

$$S_1 = \mu_u A_1, \tag{2}$$

$$S_2 = \alpha_1 A_2 + \alpha_2 A_1^2, \tag{3}$$

where α_j ($j = 1,2$) and μ_u are material constants and coefficient of viscosity respectively. $A_j (j = 1,2)$ are Rivlin-Ericksen tensors defined by

$$A_1 = (gradq) + (gradq)^t, \tag{4}$$

$$A_2 = \frac{d}{dt} A_1 + A_1 gradq + (gradq)^t A_1, \tag{5}$$

where the superscript t is the transpose of a matrix, q is the velocity field in two-dimensional flow which can be expressed as

$$q = (u(x, y, t), v(x, y, t), 0) \tag{6}$$

By examining the boundary layer, the steady state of a two-dimensional governing equations of fluid flow are [27]:

$$\frac{\partial u}{\partial x} + \frac{\partial v}{\partial y} = 0, \tag{7}$$

$$\begin{aligned} u\frac{\partial u}{\partial x} + v\frac{\partial u}{\partial y} = \nu\frac{\partial^2 u}{\partial y^2} + \frac{\alpha_1}{\rho}\left[\frac{\partial}{\partial x}\left(u\frac{\partial^2 u}{\partial y^2}\right) + v\frac{\partial^3 u}{\partial y^3} + \frac{\partial u}{\partial y}\frac{\partial^2 v}{\partial y^2}\right] \\ + [g\beta_T(T - T_\infty) + g\beta_C(C - C_\infty)] - \frac{\sigma B_0^2}{\rho}u - \frac{\nu}{K'}u \end{aligned} \tag{8}$$

$$u\frac{\partial T}{\partial x} + v\frac{\partial T}{\partial y} = \alpha\frac{\partial^2 T}{\partial y^2} + \frac{K}{\rho C_p}\left(\frac{\partial u}{\partial y}\right)^2 - \frac{1}{\rho C_p}\frac{\partial q_r}{\partial y} + \frac{\nu}{K'}u^2, \tag{9}$$

$$u\frac{\partial C}{\partial x} + v\frac{\partial C}{\partial y} = D\frac{\partial^2 C}{\partial y^2}, \tag{10}$$

with the associated boundary conditions:

$$\begin{aligned} v = 0, u = u_w = cx, T = T_w (= T_\infty + A_1 x^s), C = C_w (= C_\infty + B_1 x), \text{at } y = 0, \\ u \to 0, \frac{\partial u}{\partial y} \to 0, T \to T_\infty, C \to C_\infty, \text{as } y \to \infty. \end{aligned} \tag{11}$$

where u and v, respectively, account to the velocity components along the x and y directions. β_T, β_C, C_p, K, ν, ρ, g, σ, K', α and D represents the coefficient of thermal expansion, solutal expansion, the specific heat of a fluid at a steady pressure, thermal conductivity, kinematic viscosity, density of the fluid, acceleration due to gravity, electrical conductivity, permeability of porous medium, thermal diffusivity, and mass diffusivity respectively.

The following similarity transformations are utilized for transforming Equations (7)–(10) into an array of ordinary differential equations.

$$\psi(x, y) = \sqrt{c\nu}xF(\eta), \eta = \sqrt{\frac{c}{\nu}}y, \Theta(\eta) = \frac{T - T_\infty}{T_w - T_\infty}, \zeta(\eta) = \frac{C - C_\infty}{C_w - C_\infty} \tag{12}$$

The momentum, energy, and concentration equations are transformed into the

subsequent system of ODEs using the transformations described above:

$$F''' - (F')^2 + FF'' + k\left[2F'F''' - (F'')^2 - FF^{iv}\right] - MF' - \epsilon F' + \lambda[\Theta + N\zeta] = 0, \tag{13}$$

$$\Theta''\left(1 + \frac{4}{3}R\right) + Pr(F\Theta' - 2F'\Theta) + PrEc(F'')^2 + \epsilon F'^2 = 0, \tag{14}$$

$$\zeta'' + ScF\zeta' - ScF'\zeta = 0, \tag{15}$$

with the boundary conditions:

$$F(0) = 0, F'(0) = 1, \Theta(0) = 1, \zeta(0) = 1,$$
$$F'(\eta) \to 0, F''(\eta) \to 0, \Theta(\eta) \to 0, \zeta(\eta) \to 0 \; as \; \eta \to \infty \tag{16}$$

where, prime represents differentiation with respect to similarity variable η.

$k = \frac{\alpha_1 c}{\rho\nu}$, $M = \frac{\sigma B_0^2}{\rho c}$, $\epsilon = \frac{\nu}{K\prime c}$, $\lambda = \frac{g\beta_T(T_w - T_\infty)}{c^2 x}$, $N = \frac{\beta_C(C_w - C_\infty)}{\beta_T(T_w - T_\infty)}$, $Pr = \frac{\nu}{\alpha}$, $Ec = \frac{c^2}{AC_p}$, $Sc = \frac{\nu}{D}$ and $R = \frac{4\sigma^* T^3}{\alpha k^* \rho C_p}$ are the Visco-elastic parameter, Magnetic parameter, porosity parameter, mixed convection parameter, buoyancy ratio parameter, Prandtl number, Eckert number, Schmidt number, and radiation parameter respectively.

The skin friction coefficient C_f, local Nusselt number Nu_x, and local Sherwood number Sh_x are the physical quantities that are significant in our current topic since they have been used across engineering and industrial processes. These are described as

$$C_f = \frac{\tau_w}{\rho U_w^2}, Nu_x = \frac{x p_w}{K(T_w - T_\infty)}, Sh_x = \frac{p_m x}{D(C_w - C_\infty)}. \tag{17}$$

where τ_w, p_w and p_m are the shear stress or skin friction along the surface of the sheet defined, heat flux and mass flux respectively are given by:

$$\tau_w = \mu\left(\frac{\partial u}{\partial y}\right)_{y=0}, p_w = -k\left(\frac{\partial T}{\partial y}\right)_{y=0}, p_m = -D\left(\frac{\partial C}{\partial y}\right)_{y=0}. \tag{18}$$

Inputting Equation (20) into Equation (19), we obtain:

$$F''(0) = (Re_x)^{\frac{1}{2}} C_f, -\Theta'(0) = (Re_x)^{\frac{1}{2}} Nu_x, -\zeta'(0) = (Re_x)^{\frac{1}{2}} Sh_x. \tag{19}$$

where, $Re_x = \frac{u_w x}{\nu}$ is the local Reynolds number.

3. Numerical approach

The two primary finite difference codes for solving systems of ordinary differential equations in MATLAB are bvp4c and bvp5c. The bvp4c numerical approach is one of the most widely used approaches in MATLAB for solving coupled differential equations. The numerical approach of the bvp4c code, which we are applying in the present scenario, might be broken down into multiple steps. Using similarity transformations and dimensionless variables, Equations (7)–(10) and their boundary conditions are transformed into ODEs in the preliminary phases. In the subsequent stage, Equations (13)–(15) are transformed into a new system of first-order ordinary differential equations.

Beginning with initial key guesses, a system of equations with boundary conditions is solved. The result of this problem can be displayed on a graph. Tables will display the values for the Nusselt number and the Sherwood number, and comparative data will be interpreted.

4. Results and discussion

4.1. Magnetic effect on physical quantities

Due to the Lorentz force's influence on the flowing fluid in **Figure 1a**, velocity decreases at increasing amounts of magnetic field M = 0.0, 0.3, and 0.6. As shown in **Figures 1b** and **1c**, the opposite effect, i.e., a rise in temperature and fluid concentration, can be observed when the magnetic field is increased.

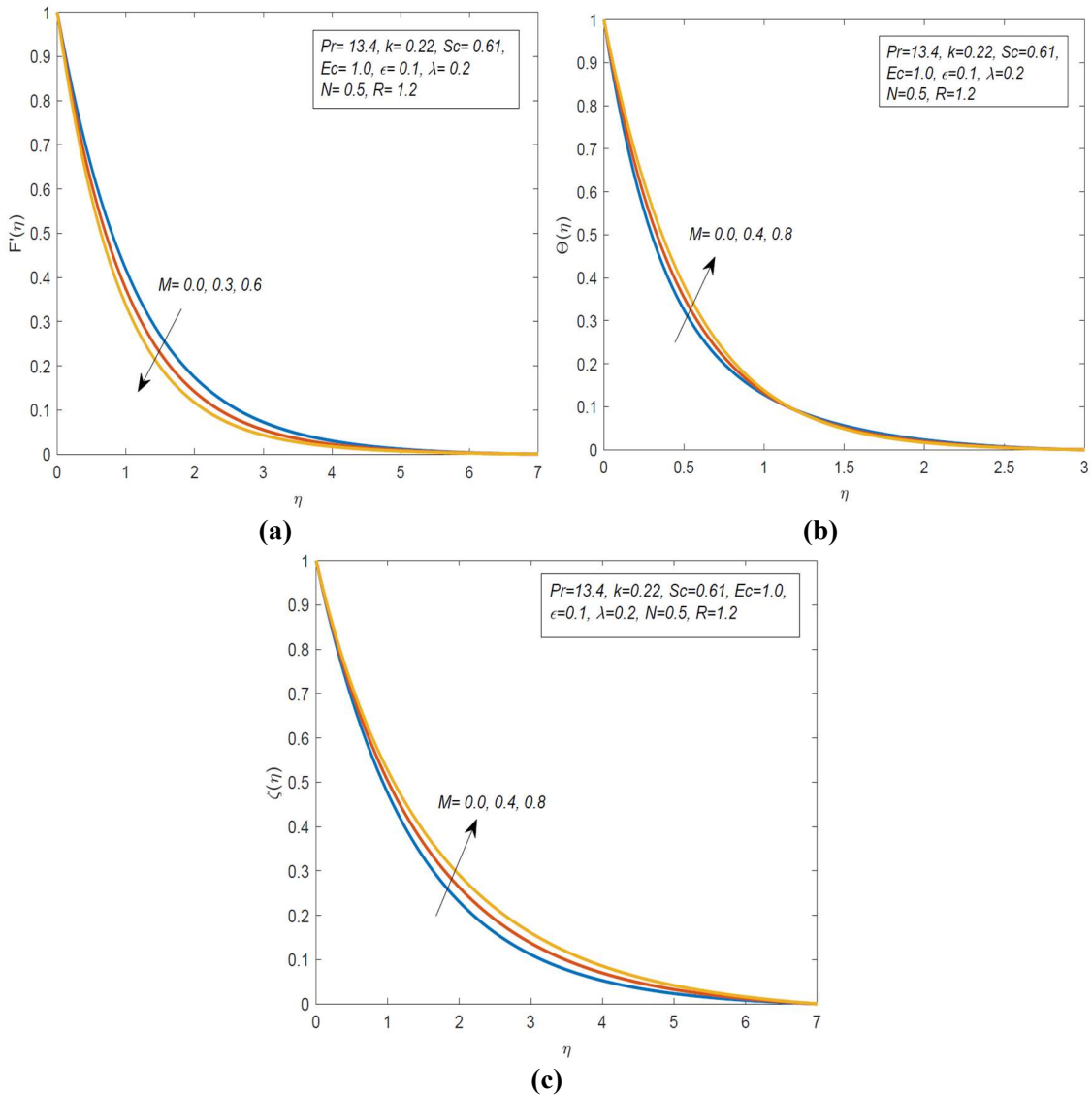

Figure 1. Effect of magnetic parameter on **(a)** velocity **(b)** temperature and **(c)** concentration.

4.2. Thermal radiation and viscoelastic effect on physical quantities

Because thermal radiation is brought on by the thermal motion of fluid particles, the temperature of the fluid rises with increasing thermal radiation parameters R = 0.0, 1.0, and 2.0, as illustrated in **Figure 2**. The interaction involving velocity and temperature is examined in **Figures 3a** and **3b**. The increasing values of k = 0.1, 0.3, and 0.5, which represent higher deformation rates, demonstrate that velocity climbs and reaches zero at about η = 2.5. Temperature decreases by growing

k in the range $0 \leq k \leq 0.7$ but increases in the range $0.8 \leq k \leq 1.8$ because it has both elastic and viscous properties.

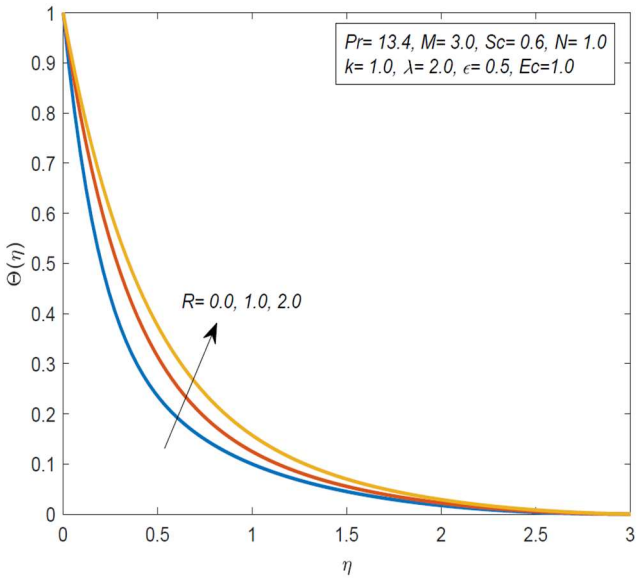

Figure 2. Effect of radiation parameter on temperature.

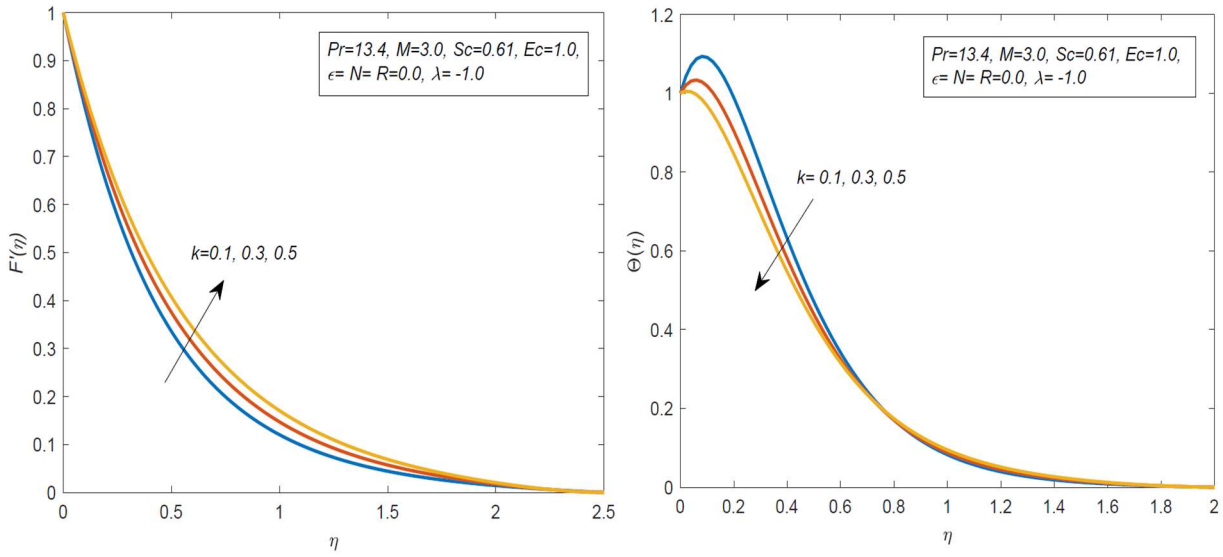

(a) **(b)**

Figure 3. Effect of viscoelastic parameter on **(a)** velocity and **(b)** temperature.

4.3. Porous and buoyancy ratio parameter on physical quantities

The porosity parameter ϵ is inversely proportional to the permeability of the porous medium K'. This leads to a reduction in the velocity profile and an inclination in the concentration profile, as depicted in **Figures 4a** and **4b**. The parameter buoyancy reflects the upward force present in the flowing fluid. By increasing the buoyancy ratio parameter N to values of 0.0, 1.0, and 2.0, fluid velocity increases, as shown in **Figure 5a**. However, the temperature profile exhibits a reverse tendency, as seen in **Figure 5b**.

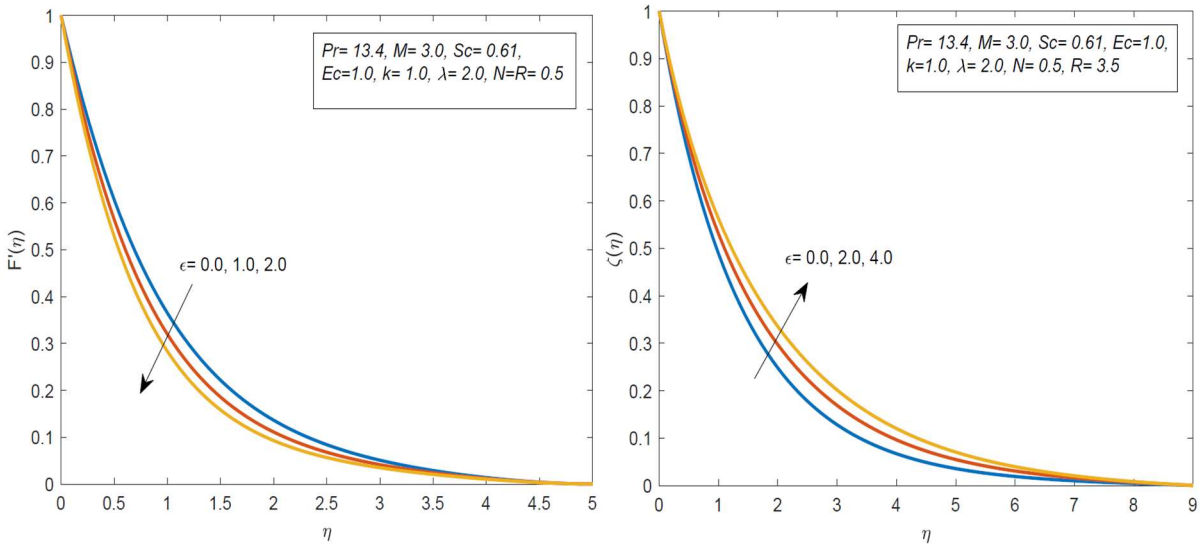

(a) **(b)**

Figure 4. Effect of porous parameter on **(a)** velocity and **(b)** concentration.

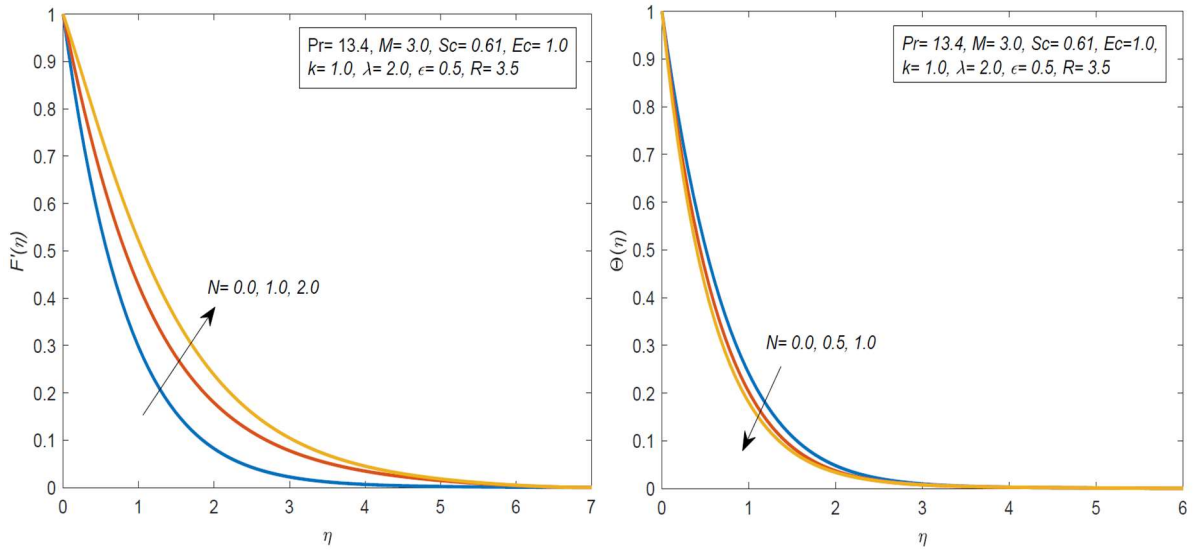

(a) **(b)**

Figure 5. Effect of buoyancy ratio parameter on **(a)** velocity and **(b)** temperature.

4.4. Schmidt number impact on physical quantities

The dimensionless Schmidt number *Sc*, stands for the ratio of momentum to mass diffusivity, and the same pattern can be seen for both velocity and concentration profiles as shown in **Figures 6a** and **6b**, i.e., decreasing when *Sc* = 0.5, 1.0, and 1.5 for velocity and *Sc* = 0.45, 0.55, and 0.65 for concentration.

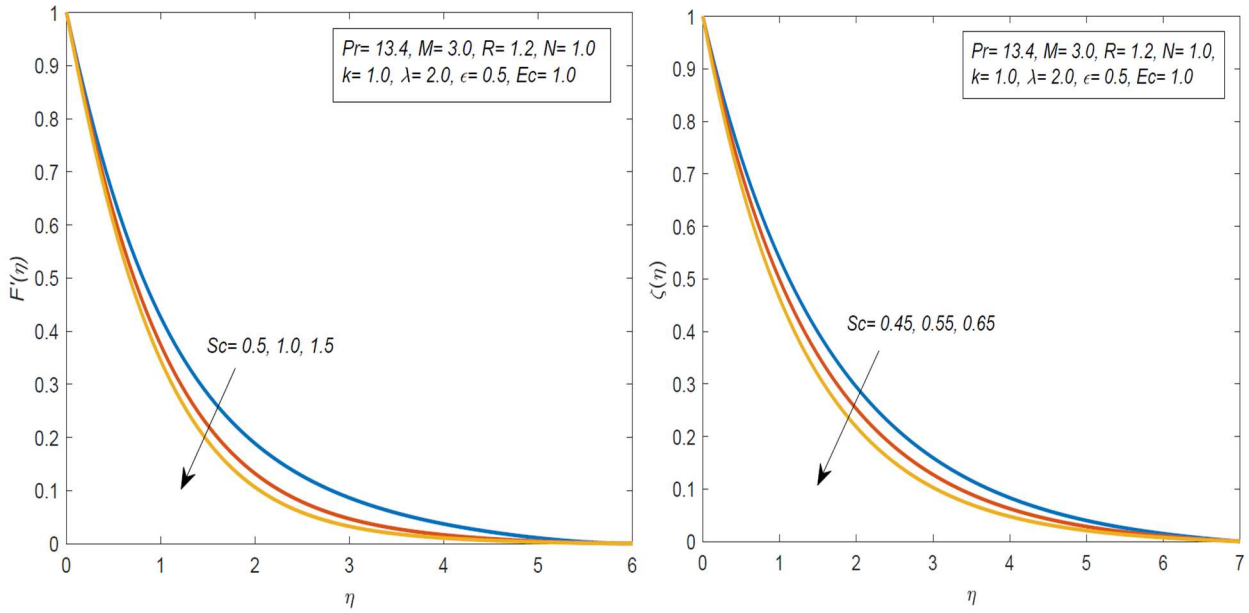

(a) **(b)**

Figure 6. Effect of Schmidt number on **(a)** velocity and **(b)** concentration.

4.5. Impact of physical parameters on Nusselt and Sherwood numbers

The Nusselt and Sherwood numbers, which depict heat and mass transport in a flowing fluid, respectively, are the other two physical measurements of relevance in this study. These studies will be shown in **Tables 1** and **2**, and their error is made noticeable when comparing them to the results of earlier investigations. **Table 1** shows the Nusselt number $-\Theta'(0)$ for various values of η and k when the Prandtl number is supposed to be one. For k = 0.01 and various η values, the Nusselt number increases, and a similar pattern has been observed for k = 0.05. The obtained results demonstrate good agreement with the analytical findings of Ghadikolaei et al. [27]. The obtained results of the Sherwood number $-\zeta'(0)$ using the shooting technique for various values of *Pr* and *Sc* in **Table 2** by setting k = 0.01, M = 2, Ec = 1 while leaving the other parameter values.

Table 1. Comparison of numerical results of Nusselt number $(-\Theta'(0))$ for different values of visco-elastic parameter (k) and similarity variable η when $R = 0$, $N = 0$, $Pr = 1$, $Sc = 0$, $\lambda = 0$, $\epsilon = 0$, $Ec = 0$ and $M = 0$.

Value of 'k'	η	Dey and Borah (first solution) [26]	Ghadikolaie et al. [27]	Present results
	0	1.3278	1.334722	1.3337
0.01	0.1	1.1627	1.150370	1.1477
	0.2	0.9963	0.993877	0.99001
	0	1.3393	1.340277	1.3388
0.05	0.1	1.1738	1.155672	1.1526
	0.2	0.9953	0.998583	0.9946

Table 2. Numerical results of Sherwood number ($-\zeta'(0)$) for different values of Prandtl number (Pr) and Schmidt number (Sc) when $R = 0$, $N = 0$, $k = 0.01$, $\lambda = 0$, $\epsilon = 0$, $Ec = 1$ and $M = 2$.

Pr	***Sc***	$-\zeta'(0)$
0.015	0.22	0.3497
7	0.22	0.3510
13.4	0.30	0.4031
13.4	0.60	0.5962

5. Conclusions

We employed MHD and thermal radiation to study the flow of second-grade fluid across a stretching sheet. When compared to the analytical results, the error is estimated. An analogous correlation between temperature and concentration is revealed by the magnetic field variance. It is found that when the magnetic field increases (= 0, 0.3, 0.6), the flow's velocity gradually decreases and becomes zero when $\eta \geq 7$. While comparing the numerical results with the studies of Ghadikolaei et al. [27], one of the primary investigations in this research. **Table 2** clearly shows that by treating Prandtl number 13.4 and increasing Sc from 0.30 to 0.60, the mass transfer rate increases from 0.4 to 0.59. Graphical observations reveal that both velocity and concentration diminish with increasing values of the Schmidt number. It is crucial to remember that the results of future research using various effects and other numerical approaches may differ from those of the current study. The other numerical methods may give more approximate results compared to the bvp4c technique, which is one of the limitations of this study. Various numerical and analytical methods can be used to determine the errors of physical quantities of interest.

Author contributions: Conceptualization, KGC and BPM; methodology, KGC; software, KGC; validation, KGC, and BPM; formal analysis, BPM; investigation, KGC; resources, BPM; data curation, KGC; writing—original draft preparation, KGC; writing—review and editing, KGC; visualization, BPM; supervision, BPM; project administration, BPM. All authors have read and agreed to the published version of the manuscript.

Conflict of interest: The authors declare no conflict of interest.

References

1. Misra J, Patra M, Misra S. A non-Newtonian fluid model for blood flow through arteries under stenotic conditions. Journal of biomechanics. 1993; 26(9): 1129-1141. doi: 10.1016/S0021-9290(05)80011-9
2. Jacobson BO, Hamrock BJ. Non-Newtonian Fluid Model Incorporated into Elastohydrodynamic Lubrication of Rectangular Contacts. Journal of Tribology. 1984; 106(2): 275-282. doi: 10.1115/1.3260901
3. Crane LJ. Flow past a stretching plate. Zeitschrift für angewandte Mathematik und Physik ZAMP. 1970; 21(4): 645-647. doi: 10.1007/bf01587695
4. Sakiadis BC. Boundary-layer behavior on continuous solid surfaces: I. Boundary-layer equations for two-dimensional and axisymmetric flow. AIChE Journal. 1961; 7(1): 26-28. doi: 10.1002/aic.690070108
5. Sakiadis BC. Boundary-layer behavior on continuous solid surfaces: II. The boundary layer on a continuous flat surface.

AIChE Journal. 1961; 7(2): 221-225. doi: 10.1002/aic.690070211
6. Hamad MAA. Analytical solution of natural convection flow of a nanofluid over a linearly stretching sheet in the presence of magnetic field. International Communications in Heat and Mass Transfer. 2011; 38(4): 487-492. doi: 10.1016/j.icheatmasstransfer.2010.12.042
7. Wang CY. Analysis of viscous flow due to a stretching sheet with surface slip and suction. Nonlinear Analysis: Real World Applications. 2009; 10(1): 375-380. doi: 10.1016/j.nonrwa.2007.09.013
8. Khan JA, Mustafa M, Hayat T, et al. On Three-Dimensional Flow and Heat Transfer over a Non-Linearly Stretching Sheet: Analytical and Numerical Solutions. Rao Z, ed. PLoS ONE. 2014; 9(9): e107287. doi: 10.1371/journal.pone.0107287
9. Hayat T, Muhammad T, Shehzad SA, et al. An analytical solution for magnetohydrodynamic Oldroyd-B nanofluid flow induced by a stretching sheet with heat generation/absorption. International Journal of Thermal Sciences. 2017; 111: 274-288. doi: 10.1016/j.ijthermalsci.2016.08.009
10. Tzirtzilakis EE, Tanoudis GB. Numerical study of biomagnetic fluid flow over a stretching sheet with heat transfer. International Journal of Numerical Methods for Heat & Fluid Flow. 2003; 13(7): 830-848. doi: 10.1108/09615530310502055
11. Datti PS, Prasad KV, Subhas Abel M, et al. MHD visco-elastic fluid flow over a non-isothermal stretching sheet. International Journal of Engineering Science. 2004; 42(8-9): 935-946. doi: 10.1016/j.ijengsci.2003.09.008
12. Schmitt RW. Double Diffusion in Oceanography. Annual Review of Fluid Mechanics. 1994; 26(1): 255-285. doi: 10.1146/annurev.fl.26.010194.001351
13. Turner JS. Double-Diffusive Phenomena. Annual Review of Fluid Mechanics. 1974; 6(1): 37-54. doi: 10.1146/annurev.fl.06.010174.000345
14. Turner JS. Double-diffusive intrusions into a density gradient. Journal of Geophysical Research: Oceans. 1978; 83(C6): 2887-2901. doi: 10.1029/jc083ic06p02887
15. Hayat T, Ahmed N, Sajid M, et al. On the MHD flow of a second grade fluid in a porous channel. Computers & Mathematics with Applications. 2007; 54(3): 407-414. doi: 10.1016/j.camwa.2006.12.036
16. Vajravelu K, Rollins D. Hydromagnetic flow of a second grade fluid over a stretching sheet. Applied Mathematics and Computation. 2004; 148(3): 783-791. doi: 10.1016/S0096-3003(02)00942-6
17. Bafakeeh OT, Raghunath K, Ali F, et al. Hall Current and Soret Effects on Unsteady MHD Rotating Flow of Second-Grade Fluid through Porous Media under the Influences of Thermal Radiation and Chemical Reactions. Catalysts. 2022; 12(10): 1233. doi: 10.3390/catal12101233
18. Massoudi M, Vaidya A. On some generalizations of the second grade fluid model. Nonlinear Analysis: Real World Applications. 2008; 9(3): 1169-1183. doi: 10.1016/j.nonrwa.2007.02.008
19. Gowda RP, Baskonus HM, Naveen Kumar R, et al. Computational Investigation of Stefan Blowing Effect on Flow of Second-Grade Fluid Over a Curved Stretching Sheet. International Journal of Applied and Computational Mathematics. 2021; 7(3). doi: 10.1007/s40819-021-01041-2
20. Awan AU, Abid S, Ullah N, et al. Magnetohydrodynamic oblique stagnation point flow of second grade fluid over an oscillatory stretching surface. Results in Physics. 2020; 18: 103233. doi: 10.1016/j.rinp.2020.103233
21. Khan Y, Akram S, Razia A, et al. Effects of Double Diffusive Convection and Inclined Magnetic Field on the Peristaltic Flow of Fourth Grade Nanofluids in a Non-Uniform Channel. Nanomaterials. 2022; 12(17): 3037. doi: 10.3390/nano12173037
22. Kotnurkar AS, Giddaiah S. Double diffusion on peristaltic flow of nanofluid under the influences of magnetic field, porous medium, and thermal radiation. Engineering Reports. 2020; 2(2). doi: 10.1002/eng2.12111
23. Asha SK, Sunitha G. Influence of thermal radiation on peristaltic blood flow of a Jeffrey fluid with double diffusion in the presence of gold nanoparticles. Informatics in Medicine Unlocked. 2019; 17: 100272. doi: 10.1016/j.imu.2019.100272
24. Asha SK, Sunitha G. Thermal radiation and Hall effects on peristaltic blood flow with double diffusion in the presence of nanoparticles. Case Studies in Thermal Engineering. 2020; 17: 100560. doi: 10.1016/j.csite.2019.100560
25. Akbar N, Khan z, Nadeem S, et al. Double-diffusive natural convective boundary-layer flow of a nanofluid over a stretching sheet with magnetic field. International Journal of Numerical Methods for Heat & Fluid Flow. 2016; 26(1): 108-121. doi: 10.1108/hff-01-2015-0019
26. Dey D, Borah R. Stability analysis on dual solutions of second- grade fluid flow with heat and mass transfers over a stretching sheet. International Journal of Thermofluid Science and Technology. 2021; 8(2). doi: 10.36963/ijtst.2021080203

27. Ghadikolaei SS, Hosseinzadeh Kh, Yassari M, et al. Analytical and numerical solution of non-Newtonian second-grade fluid flow on a stretching sheet. Thermal Science and Engineering Progress. 2018; 5: 309-316. doi: 10.1016/j.tsep.2017.12.010
28. Endalew MF, Sarkar S. Capturing the Transient Features of Double Diffusive Thin Film Flow of a Second Grade Fluid Through a Porous Medium. International Journal of Applied and Computational Mathematics. 2019; 5(6). doi: 10.1007/s40819-019-0743-7.